



Contents lists available at ScienceDirect

Journal of Non-Crystalline Solids

journal homepage: www.elsevier.com/locate/jnoncrsol

Synchrotron XPS studies of illuminated and annealed flash evaporated a-Ge₂S₃ films

Vladimir Mitsa^a, Roman Holomb^{a,*}, Oleksandr Kondrat^a, Nataliya Popovych^a, Nataliya Tsud^b, Vladimír Matolín^b, Kevin C. Prince^c, Gabor Lovas^a, Stepan Petretskiy^a, Sára Tóth^d

^a Research Institute of Solid State Physics and Chemistry, Uzhhorod National University, Uzhhorod, Ukraine

^b Department of Surface and Plasma Science, Faculty of Mathematics and Physics, Charles University, Prague, Czech Republic

^c Elettra-Sincrotrone Trieste S.C.p.A., Trieste, Italy

^d Wigner Research Centre for Physics of the Hungarian Academy of Sciences, Budapest, Hungary

ARTICLE INFO

Article history:

Received 23 September 2013

Received in revised form 6 December 2013

Available online xxxx

Keywords:

Synchrotron radiation photoelectron spectroscopy;

XPS;

Ge₂S₃ film;

Local structure;

Thermal and laser treatment

ABSTRACT

The atomic composition, local structure and coordination of flash evaporated Ge₂S₃ films and their changes induced by laser illumination and thermal annealing in vacuum were investigated by means of high resolution synchrotron radiation and X-ray photoelectron spectroscopy. The top surface and subsurface layers of the films are found to be enriched by Ge in comparison with the composition of target glass and contain oxygen and a significant contribution of physisorbed carbon. The influence of laser and thermal treatments of flash evaporated Ge–S films in vacuum on their composition is analyzed. The local atomic coordination obtained by curve fitting of Ge 3d, S 2p, O 1s and C 1s core level spectra is discussed in detail.

© 2013 Elsevier B.V. All rights reserved.

1. Introduction

Nonlinearities of As₂S₃ chalcogenide glass are as high as 100× that for fused silica and can be applied to all-optical switching [1,2]. Replacing of As by Ge atoms raises the linear index of refraction measured at 630 nm from 2.61 (As₂S₃) to 2.75 (Ge₂S₃) [3]. In accordance with the empirical Miller law [4] the enhancement of optical nonlinearity in such Ge-rich film is expected. This opens up possibilities for their use as the active element in all-optical switching devices. It is well known that composition, structure and properties of films are depending from deposition techniques and condition of condensation. Due to the lack of periodicity in their structure their density is lower than that of the corresponding crystals, which contributes to their high sorption. The dangling bonds occurred in the fresh film that are easy to saturate when the film was exposed to air and reacted with oxygen. XPS study has confirmed the presence of As₂O_x oxides at the surface of as-patterned As₂S₃ waveguides exposed to ambient condition for just a few hours. These As₂O₃ crystals can have a devastating effect on propagating light by introducing a major source of scattering loss in submicron optically integrated circuits [5].

The properties of a-As₂S₃ film prepared by thermal evaporation, flash evaporation and magnetron sputtering are different, approaching to those found in bulk glass in the later two cases. With respect to optical and non-linear optical applications of Ge₂S₃ film it is very important to characterize the local structure and composition at the surface of the film in order to find the optimal method and condition of preparation and to investigate the possibility of subsequent modification of the material structure and properties e.g. by thermal or laser treatments.

Recently during the investigation of oxysulfide GeS₂–GeO₂ films [6] it has been found that preparation of 20 nm thick a-GeS₂ film by magnetron sputtering is accompanied by the formation of a thin layer on top of the film with lower index of refraction with respect to the bulk. In Ref. [7] we assumed that the visible photoluminescence (PL) peak at 2.2–2.3 eV might arise from GeO_x impurities in the structure of GeS₂-based glasses. In such glasses the main peak in PL spectra at 1.96 eV was identified with sulfide-dominated dopant sites, while the shoulder at 2.02 eV was attributed to oxide-dominated sites [8]. The mechanism of luminescence in Ge-based amorphous and nanocrystalline materials is still being disputed [9,10]. It is found that large PL signals correlate with good interface properties [11]. Laser illumination and thermal annealing might be employed in order to get high quality chalcogenide glassy (ChG) films [12]. Here, we report the surface characterization of Ge₂S₃ films within the few top nanolayers. It was carried out with high resolution synchrotron radiation photoelectron spectroscopy (SRPES). Deeper

* Corresponding author. Tel.: +380 31 22 33020; fax: +380 31 22 32339.

E-mail address: holomb@ukr.net (R. Holomb).

layers up to 3 nm were investigated by ordinary X-ray photoelectron spectroscopy (XPS).

2. Materials and methods

The Ge_2S_3 bulk glass was synthesized using 99.999% elemental Ge and purified S. The weighted Ge and S mixture then was sealed in evacuated ($\sim 10^{-3}$ Pa) dry quartz ampoules and stepwise gradually heated up to 1223 K in a rocking furnace. At the end of the process each ampoule was quenched at room temperature. Films were obtained by flash evaporation of glassy powder onto c-Si substrate. The irradiation of films was carried out in ultra high vacuum (UHV) at room temperature for ~ 1 h by a diode laser operating at 532 nm of 100 mW/cm^2 intensity. The photon energy of 2.33 eV (532 nm) is slightly higher than optical bandgap reported for a- Ge_2S_3 film (2.16 eV) [3]. Thermal annealing was performed for 30 min in UHV at 320°C ($T_g - 30^\circ$). Although the material treatments (laser irradiation and thermal annealing) have been performed at UHV the samples have been contacted with air during insertion in experimental chamber.

Photoemission measurements were performed at the Materials Science Beamline of the Elettra Synchrotron light source (Trieste, Italy). The spectrometer was calibrated with the Au $4f_{7/2}$ photoemission line at 84.0 eV from an evaporated gold film. The S 2p, Ge 3d, C 1s and O 1s core level peaks were fitted using a Voigt function with subtraction of a Shirley type background to yield peak position and intensity. The statistical branching ratios of 2:1 and 3:2 were used for the spin-orbit split S 2p (2p $_{3/2}$ and 2p $_{1/2}$) and Ge 3d (3d $_{5/2}$ and 3d $_{3/2}$) core level intensities, respectively. Doublet separations of 1.18 and 0.60 eV were used for S 2p and Ge 3d core levels, respectively. Other details of measurements and curve fitting were the same as described in our previous articles [13,14].

3. Results

In order to examine the vibrational modes of Ge_2S_3 -based films [15,16] a complementary technique, SRPES and ordinary XPS spectroscopy, was used to characterize the GeO_x and GeS_x species on the surface. SRPES and XPS measurements have been performed on the as-deposited, illuminated and annealed films. The study was carried out by analyzing the Ge 3d, S 2p, O 1s and C 1s core levels of Ge_2S_3 glass and evaporated thin films. The binding energy values of different germanium sulfide [17–19] and oxide [20,21] compounds were used as reference energies during SRPES and XPS data treatment. Fig. 1 shows the Ge 3d and S 2p SRPES spectra of flash evaporated Ge_2S_3 films before (top) and after (bottom) thermal annealing together with the curve fitting results. As can be seen the intensity of Ge 3d and S 2p significantly increase after thermal annealing in vacuum while laser irradiation did not affect the spectra much (not shown). Component analysis shows that the GeS- and ethane-like, $\text{GeS}_{4/2}$, GeO_x and GeO_2 species were detected in the Ge 3d spectra of as deposited film. The drastic changes in the local structure of the material were found after thermal annealing in UHV. As can be seen in Fig. 1 the Ge 3d spectra of annealed film contain three components only. The GeS-like and ethane-like species with Ge–Ge bonds disappeared and the intensities of GeO_x and GeO_2 components simultaneously increase. According to S 2p spectra the surface of both amorphous and annealed Ge_2S_3 film contains $(\text{S}_2)^{2-}$ defects, S–Ge bonds together with S_n species. The thermal annealing in UHV leads to the formation of addition S_n chains.

The contaminant atoms namely carbon and oxygen were also observed on the top of sample surface. Fig. 2 demonstrates the C 1s and O 1s core level spectra of Ge_2S_3 films and their changes due to thermal annealing. The components obtained from the curve fitting are indicated in the figure. As mentioned above for the Ge and S atoms the laser irradiation in vacuum does not change significantly the concentration

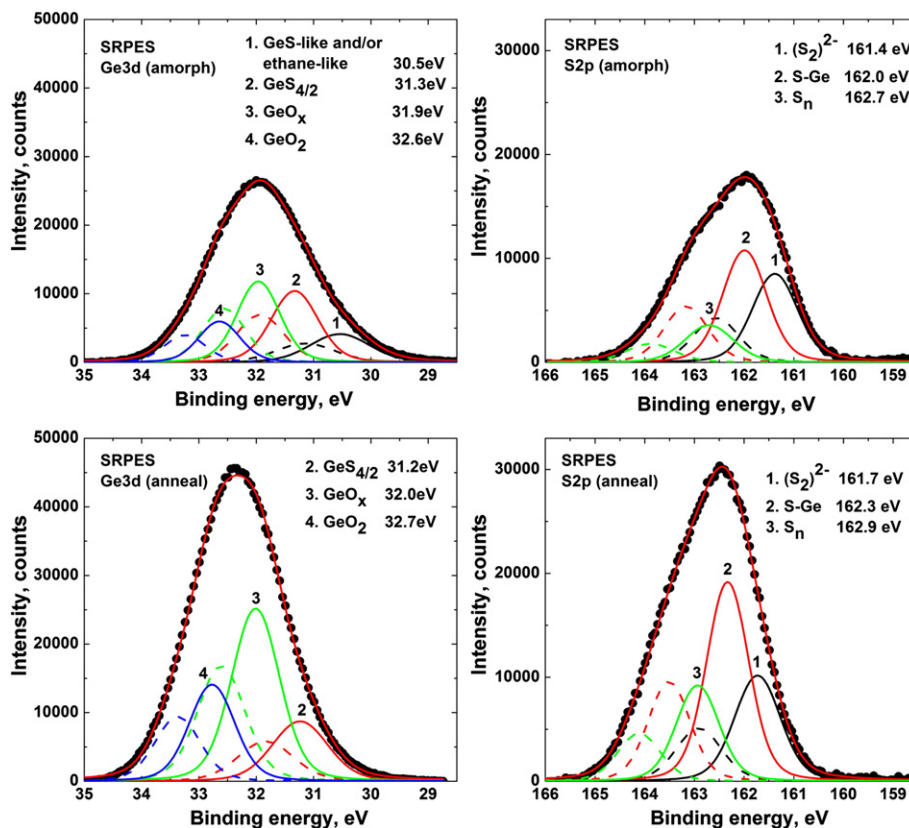


Fig. 1. Ge 3d and S 2p SRPES spectra of flash evaporated Ge_2S_3 films before (top) and after (bottom) thermal annealing.

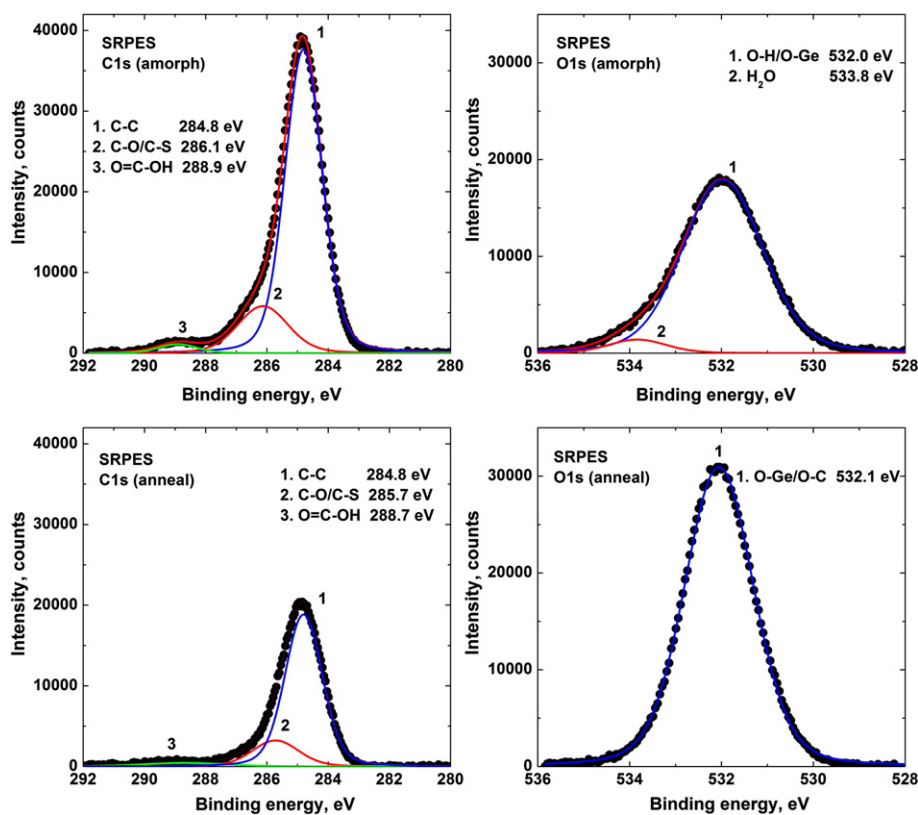


Fig. 2. C 1s and O 1s SRPES spectra of flash evaporated Ge_2S_3 films before (top) and after (bottom) thermal annealing.

and chemical bonding of the contaminant atoms. The drastic decreasing in intensity of C 1s signal after thermal annealing is accompanied with the increasing of Ge 3d and S 2p signals. Therefore we assumed that physisorbed carbon desorbs from the sample surface during thermal processes in UHV. The increase of the O 1s peak intensity after annealing is in agreement with the increasing Ge 3d and S 2p peak intensities.

4. Discussion

4.1. Atomic composition and its changes

The surface and subsurface composition of the amorphous, annealed and illuminated Ge_2S_3 films is shown in Table 1. Compositional analysis shows that the top surface (measured by SRPES) of as-deposited film is depleted by chalcogen. In this case the Ge to S ratio is 1.33 which is relatively high in comparison with the target glass powder (0.67).

The oxygen and the significant amount of carbon were also detected on the film surface. XPS measurements show lower Ge to S ratio (1.00) and higher concentration of oxygen atoms. Taking into account that the XPS method integrates structural information both from top surface and deeper layers it can be concluded that the Ge to S ratio in deeper layers is closer to that found in target material in comparison with top layers

Table 1

Composition (atomic%) obtained by SRPES (615 eV) and ordinary XPS (1486.6 eV) analysis for the different elements of amorphous films obtained by flash evaporated $\text{Ge}_{40}\text{S}_{60}$ glass powder.

Sample	Energy, eV	Ge, %	S, %	C, %	O, %	Ge/S
As deposited	615	20	15	52	13	1.33
Irradiated	615	19	14	54	13	1.35
Annealed	615	32	25	25	18	1.29
As deposited	1486.6	17	17	40	26	1.00
Irradiated	1486.6	14	14	41	31	1.00
Annealed	1486.6	23	24	24	29	0.95

which are very affected by surface processes. As can be seen the laser irradiation in vacuum leads only to small changes in atomic composition. The minor increase in Ge to S ratio after illumination is detected only by SRPES i.e. at the top surface layers (see Table 1). Results show that more changes in composition are taking place after thermal annealing of the sample. The significant increases of Ge 3d, S 2p and O 1s peak intensities are accompanied with the simultaneous decreases of C 1s peak intensity. The carbon content is found to decrease approx. twice upon 30 min thermal annealing in UHV which can be related to thermal desorption of physisorbed carbon from the surface. At the same time the decrease of Ge to S ratio was observed both by SRPES and XPS methods.

4.2. Local structure and component analysis

The analysis of the components of Ge 3d and S 2p core level spectra obtained from the fitting procedure (Fig. 1) and their structural assignment is presented in Tables 2 and 3, respectively. The analysis of Ge 3d spectra (Fig. 1, Table 2) of Ge–S film shows that the thermal annealing leads to the increase of concentration of GeO_x and GeO_2 species. The concentration of $\text{GeS}_{4/2}$ s.u. which is the main component found in bulk Ge_2S_3 glass (see Tab. 4 in [22]) is decreasing during thermal annealing of the film. In contrast with the bulk glass the ethane- ($\text{S}_3\text{Ge}-\text{GeS}_3$) and GeS-like s.u. were not detected in the structure of annealed film. On the other hand, the significant contribution of Ge-oxides at film surface was detected. It leads to the separation of sulfur-rich (dimers and chains) s.u. on the surface (Fig. 1, Table 3). Only negligible small concentration of such S-dimers was detected by XPS method.

The C 1s signal was associated mainly with the surface and near-surface region. Carbon is partially removed from the surface and near surface during the annealing process in UHV at temperature T_g-30° (Fig. 2, Table 1).

In an earlier XPS investigation of Ge_2S_3 -based films the carbon contamination (an atomic percentage of about 15–20%) has always been determined but was not taken into account during the consideration

Table 2

Individual components determined from curve fitting of Ge 3d spectra as evaporated, irradiated and annealed Ge–S films (Fig. 1) and their contribution (area, %). The main ($3d_{5/2}$) peak of each doublet is considered.

Peak number	Core level/ component	As evaporated sample, peak area, %	Irradiated sample peak area, %	Annealed sample peak, area, %
<i>Ge 3d, 615 eV</i>				
Peak 1	GeS-like and/ or ethane-like	17	13	–
Peak 2	GeS _{4/2}	33	32	19
Peak 3	GeO _x	34	37	51
Peak 4	GeO ₂	16	18	30
<i>Ge 3d, 1486.6 eV</i>				
Peak 1*	Ge _{4/4}	–	2	–
Peak 1	GeS-like and/ or ethane-like	25	22	–
Peak 2	GeS _{4/2}	43	46	20
Peak 3	GeO _x	30	30	60
Peak 4	GeO ₂	2	–	20

of surface composition [23]. It can be noted as well, that in Auger spectra of ternary ChG film during long term aging, the tail of carbon and oxygen signals extended up to 30 nm in depth [24], but 10–20 nm are below the detection limit in the Auger profile. In our case laser illumination of a thin film in vacuum leads to small changes of Ge/S ratio on the surface (Table 1). Also, the illumination with energy above the bandgap results in the breakdown of Ge–S bonds and creation of new Ge–O bonds in the irradiated area on the top of the film (Table 2). The analysis of SRPES Ge 3d spectra has shown that after thermal annealing the concentration of GeO₂ and GeO_x on top is reduced. Nearly the same effect is observed for the deeper layers as confirmed by the XPS peak signal from 3 nm (Table 2). In previous literature for Ge₂₅Ga₁₀S₆₅ glasses studied by XPS and X-ray absorption spectroscopy (XAS), a similar situation can be found [20]. XPS data showed that Ge_{4/4} exists in small quantities in the deeper layers of the illuminated zone and might be connected with the fact that part of the germanium oxides decompose into Ge_{4/4} s.u. after illumination [21]. As already stated, on the basis of our previous investigations, the Ge_{4/4} s.u. were found in the illuminated zone too, during measurement of Raman spectra which confirmed the XPS spectra assignment (Table 2) [15]. It is known that the evaporation of Ge-based glasses is often a non-congruent vaporization process which can lead to the formation of off-stoichiometry films [11]. In [19] the composition of the thermally deposited film based on Ge₄₀S₆₀ glass was determined as Ge₄₆S₅₄ and did not match well with that of the bulk glass. During fitting of SRPES and XPS spectra of C 1s core level peak (not shown here) there is no indication of Ge–C bond formation (binding energy 284.3 eV [25]). Apart from the main peak associated with C–C/C–H bonds (284.8 eV) the only C–S and/or C–O bonds were found at

Table 3

Individual components determined from curve fitting of S 2p spectra as evaporated, irradiated and annealed Ge–S films (Fig. 1) and their contribution (area, %). The main ($2p_{3/2}$) peak of each doublet is considered.

Peak number	Core level/ component	As evaporated sample, peak area, %	Irradiated sample peak area, %	Annealed sample peak, area, %
<i>S 2p, 615 eV</i>				
Peak 1	(S ₂) ^{2–}	37	34	28
Peak 2	S–Ge	46	47	48
Peak 3	S _n	17	19	24
<i>S 2p, 1486.6 eV</i>				
Peak 1	(S ₂) ^{2–}	–	–	11
Peak 2	S–Ge	87	79	70
Peak 3	S _n	13	21	19

–286 eV. That is why we consider the structural composition of Ge₂S₃ films on the surface and subsurface as GeS₂ × Ge_{1–x}S_x × GeO₂ × GeO_y ($x < 0.6, y < 2$). The ratio GeS₂ × Ge_{1–x}S_x/GeO₂ × GeO_y (see data in Table 2) on the surface of films before illumination is near 1 and drastically differs from that found in bulk sample with freshly polished surface [22].

We suggested that oxidation of Ge might play an important role in radiative recombination processes on the surface of Ge₂S₃-based films and it needs further investigations. The results obtained are the evidence that annealing transform the Ge-rich species in both the surface and subsurface regions. The local coordination in the as-evaporated Ge–S film is significantly different from the structure of bulk glass, contains the big amount of oxidized Ge species and the thermal annealing does not lead to the formation of local structure typical to those found in glass [22].

5. Conclusions

The atomic composition and local structure of flash evaporated Ge₂S₃ films and their changes during laser and thermal treatment in UHV were investigated in detail by means of synchrotron radiation and X-ray photoelectron spectroscopy. The top surface and subsurface layers of the films are found to be enriched by Ge in comparison with the composition of target glass and contain oxygen and a significant contribution of physisorbed carbon. Laser irradiation of the as-evaporated Ge–S film in UHV leads to small changes only in composition and local atomic coordination. However, the thermal annealing of the sample in UHV leads to drastic changes in the structure and local coordination: the majority of the carbon contaminant atoms desorbed from the surface, the concentration of Ge-rich Ge–S species rapidly decreases with simultaneous increase in concentration of Ge oxides. Such changes lead to the local separation of sulfur-rich components and to the formation of S_n chains. Thermal annealing of the as evaporated Ge–S film at temperature near the glass transition temperature did not move the surface toward the composition and local coordination of bulk glass.

Acknowledgments

The authors thank Dr. M. Veres (Institute for Solid State Physics and Optics, Wigner Research Center for Physics of the Hungarian Academy of Sciences) for his assistance with Raman monitoring of laser irradiation of the sample. R.H. gratefully acknowledges the support from the Hungarian Academy of Sciences within Domus Hungarica Scientiarum et Artium Programme. The Materials Science Beamline is supported by the Ministry of Education of Czech Republic under Grant No. LG 12003.

References

- [1] B. Luther-Davies, S.J. Madden, D.-Y. Choi, R.-P. Wang, A. Rode, A. Prasad, R.A. Jarvis, D.J. Moss, B.J. Eggleton, C. Grillet, M.R.E. Lamont, V.G. Ta'eed, M. Shookooh-Saremi, N. Baker, I.C. Littler, L. Fu, M. Rochette, Y. Ruan, Proceedings of the International Conference on Photonics in Switching, IEEE, 2006, pp. 158–160.
- [2] B.J. Eggleton, B. Luther-Davies, K. Richardson, Nat. Photonics 5 (2011) 141–148.
- [3] V. Mitsa, Institute of Semiconductors Physics, Doctoral Thesis NAS of Ukraine, Kyiv, 2003.
- [4] C.C. Wang, Empirical relation between the linear and the third order nonlinear optical susceptibilities, Phys. Rev. B 2 (1970) 2045–2048.
- [5] J. Hu, N.-N. Feng, N. Carlie, L. Petit, A. Agarwal, K. Richardson, L. Kimerling, Opt. Express 18 (2010) 1469–1478.
- [6] C. Maurel, T. Cardinal, P. Vinatier, L. Petit, K. Richardson, N. Carlie, F. Guillen, M. Lahaye, M. Couzi, F. Adamietz, V. Rodriguez, F. Lagugné-Labarthe, V. Nazabal, A. Royon, L. Canioni, Mater. Res. Bull. 43 (2008) 1179–1187.
- [7] V. Mitsa, R. Holomb, G. Lovas, M. Ivanda, G. Rudyko, E. Gule, I. Fekeshgazi, MIPRO Proceedings of the 35th Intern. Conf, 2012, pp. 21–22.
- [8] X. Liu, M. Naftaly, A. Iha, J. Lumin. 96 (2002) 227–238.
- [9] K. Tanaka, Phys. Status Solidi B 250 (2013) 988–993.
- [10] M. Peng, Y. Li, J. Gao, D. Zhang, Z. Jiang, X. Sun, J. Phys. Chem. C 115 (2011) 11420–11426.
- [11] Carlo Lambertini, Characterization of Semiconductor Heterostructures and Nanostructures, first ed., Elsevier Science, 2008.

- [12] R.-P. Wang, A. Rode, S. Madden, B. Luther-Davies, *J. Am. Ceram. Soc.* 90 (2007) 1269–1271.
- [13] O. Kondrat, N. Popovych, R. Holomb, V. Mitsa, V. Lyamayev, N. Tsud, V. Cháb, V. Matolín, K.C. Prince, *J. Non-Cryst. Solids* 358 (2012) 2910–2916.
- [14] O. Kondrat, N. Popovych, R. Holomb, V. Mitsa, V. Lyamayev, N. Tsud, V. Cháb, V. Matolín, K.C. Prince, *Thin Solid Films* 520 (2012) 7224–7229.
- [15] O. Gamulin, M. Ivanda, V. Mitsa, M. Balarin, M. Kosovic, *J. Mol. Struct.* 993 (2011) 264–268.
- [16] R. Holomb, P. Johansson, V. Mitsa, I. Rosola, *Phil. Mag.* 85 (2005) 2947–2960.
- [17] H. Takebe, H. Maeda, K. Morinaga, *J. Non-Cryst. Solids* 291 (2001) 14–24.
- [18] F. Mirabella, R.L. Johnson, J. Ghijsen, *Surf. Sci.* 506 (2002) 172–182.
- [19] M. Mitkova, A. Kovalskiy, H. Jain, Y. Sakaguchi, *J. Optoelectron. Adv. Mater.* 11 (2009) 1899–1906.
- [20] P.N. Lisboa-Filho, V.R. Mastelaro, W.H. Schreiner, S.H. Messaddeq, M. Siu Lib, Y. Messaddeq, P. Hammer, S.J.L. Ribeiro, P. Parent, C. Laffond, *Solid State Ionics* 176 (2005) 1403–1409.
- [21] P. Broqvist, J.F. Binder, A. Pasquarello, *Appl. Phys. Lett.* 97 (2010) 202908–202911.
- [22] V. Mitsa, M. Ivanda, O. Gamulin, R. Holomb, O. Kondrat, N. Popovych, G. Lovas, S. Petreckiy, N. Tsud, V. Matolín, K.C. Prince, *MIPRO Proceedings of the 36th Intern. Conf.* 2013, pp. 34–39.
- [23] V. Pamukchieva, E. Skordeva, D. Arsova, M.-F. Guimona, D. Gonbeau, *J. Optoelectron. Adv. Mater.* 7 (2005) 1265–1270.
- [24] T.N. Shchurova, N.D. Savchenko, K.O. Popovic, N. Yu, Baran, *Chem. phys. Technol. surf. (Ukraine)* 1 (2010) 343–347.
- [25] C.Q. Hua, W.T. Zhenga, B. Zhenga, J.J. Lia, Z.S. Jina, X.M. Baia, H.W. Tiana, Q. Jianga, X.Y. Wang, J.Q. Zhuh, S.H. Mengb, X.D. Heb, J.C. Han, *Vacuum* 77 (2004) 63–68.